Ethanol steam reforming over bimetallic coated ceramic foams: effect of reactor configuration and catalytic support

Vincenzo Palma[a,*], Concetta Ruocco[a], Filomena Castaldo[a], Antonio Ricca[a], Daniela Boettge[b]
[a] Department of Industrial Engineering, University of Salerno, Via Giovanni Paolo II 132, 83040 Fisciano (SA), ITALY
[b] Fraunhofer-Institut für Keramische Technologien und Systeme, IKTS Winterbergstrasse 28 01277 Dresden, Germany
[*]Corresponding author: +39.089.964147, cruocco@unisa.it

Abstract: In recent years, hydrogen production from renewable feed-stocks attracts particular attention. Specifically, the steam reforming of biomass-derived bioethanol could provide H_2-rich effluent stream, representing an interesting research field. This study focuses on the development of bimetallic structured catalysts, supported on ceria and ceria-zirconia, active in Ethanol Steam Reforming (ESR) reaction at low-temperature (300-600°C) and characterized by improved heat transfer properties. ESR reaction was carried out on ceramic foams and, as a comparison, on powders catalysts. In particular, catalytic test were carried out on two reactor configurations, evidencing that the better thermal management of the latter results in significantly higher conversions. The enhanced thermal conductivity of SiC foams catalysts, tested in the tubular reactor, allowed overcoming heat transfer limitations in easy reactor geometry, resulting in very good performances. Moreover, the effect of catalytic support on ethanol conversion and H_2 yield was investigated.

Keywords: Hydrogen, Ethanol-Steam-Reforming, SiC foam catalyst.

1. Introduction

One of the best way to reduce oil and gasoline depletion and green gas emissions is by encouraging clean energy production. Unlike fuel fossils, hydrogen combustion does not involve environmental pollutants and this feature, coupled to its abundance in the universe, make H_2 a suitable fuel to meet future energy supply [1]. Although the most common technologies for producing hydrogen involve thermo-catalytic processes of natural gas or heavy oils [2], sustainable generation is possible only by using environmentally friendly methods. Widely available and cheap feed-stocks, such as biomass, are expected to become preferred sources, in order to reduce energy production costs. However, direct production of hydrogen from biomass through pyrolysis and gasification technologies causes feedstock decomposition, followed by char and tar formation [3]. On the contrary, bioethanol production through hydrolysis and fermentation of biomass and its conversion to hydrogen via steam reforming seems to be a very promising alternative strategy [4-6]. In fact, C_2H_5OH is more advantageous than conventional fuels mainly for the absence of heteroatoms, such as sulphur, and neutrality of process with respect to CO_2 emission, ensuring the closure of carbon cycle [7]. Moreover, the route of feeding bioethanol to a steam reformer is very attractive, mostly due to the deeper knowledge of reforming technologies with respect to other alternative methods to produce hydrogen.

Ethanol steam reforming (Eq. 1) can theoretically provide 6 moles of H_2 per mole of reacted C_2H_5OH:

$$C_2H_5OH + 3H_2O \rightleftarrows 6H_2 + 3CO_2 \qquad \Delta H^0_{298K} = 173.5\ kJ/mol \qquad \text{Eq. 1}$$

However, the reaction system is very complex, resulting as the subsequence of several reactions (Eq. 1 to Eq. 5); simultaneously, several side-reactions could occur (Eq. 7 to Eq. 9), reducing H_2 yield and selectivity [8, 9], and resulting in catalyst deactivation.

$$C_2H_5OH \rightleftarrows H_2 + CO + CH_4 \qquad \text{Eq. 2}$$

$$CH_4 + H_2O \rightleftarrows 3H_2 + CO \qquad \text{Eq. 3}$$

$$CH_4 + 2H_2O \rightleftarrows 3H_2 + CO_2 \qquad \text{Eq. 4}$$

$$CO + H_2O \rightleftarrows H_2 + CO_2 \qquad \text{Eq. 5}$$

$$C_2H_5OH \rightleftarrows C_2H_4O + H_2 \qquad \text{Eq. 6}$$

$$C_2H_5OH \rightleftarrows C_2H_4 + H_2O \qquad \text{Eq. 7}$$

$$C_2H_4 \rightarrow 2C_{(s)} + 2H_2 \qquad \text{Eq. 8}$$

$$2CO \rightarrow C_{(s)} + CO_2 \qquad \text{Eq. 9}$$

In order to maximize hydrogen production efficiency, proper operating conditions (temperature, pressure, feeding and dilution ratios) have to be selected. As reported in Eq. 1, the ethanol steam reforming reaction is endothermic, and results in a mole number increasing, thus the reaction is

thermodynamically promoted at high operating temperature and low pressure. On the contrary, due to the Water-Gas Shift reaction (WGS) equilibrium (Eq. 5), to operate at too high temperature, could result in a not-negligible carbon monoxide production, limiting the possibility of feeding the reforming mixture to a fuel cell, since amounts of carbon monoxide higher than 10 ppm are responsible for PEMFCs poisoning [10]. In addition, increasing temperatures impact significantly on hydrogen production costs, both in term of operating and plant charges. Accordingly, the chance of performing ethanol steam reforming in the low temperature range appears particularly interesting. However, acetaldehyde and ethylene formation (Eq. 6 and Eq. 7) are favoured at relatively low temperatures and also CO dissociation to form coke (Eq. 9) easily occurs [11]. From the thermodynamic standpoint, the choice of optimal feeding conditions (water to ethanol molar ratios higher than 3) allows avoiding coke formation [12]. Moreover, low reaction temperature may negatively affect on reaction kinetics, resulting in a too slow reaction system. A proper choice of catalytic formulations may results in a selective reaction rate increasing, that in turn drives the system to a better by-products selectivity and hydrogen yield. In addition, due to the highly endothermic nature of the ESR reaction, the heat transfer rate from the heating medium to the catalytic system is one of the crucial issues for the process; therefore the role of thermal support properties requires further investigation.

Several authors studied ethanol steam reforming on oxides-supported noble and non-noble metals based catalysts [13-19]. Among non-noble metals, selected on the basis of their lower cost with respect to noble ones, cobalt and nickel showed the highest activity towards ethanol steam reforming [20]. Ni based catalysts exhibited a relevant ability in promoting C-C bonds breaking and hydrogenation/dehydrogenation reactions [21], while Co based catalysts are interesting for their low generation of CH_4 as by-product and coke [22]. However, the interaction of active species with catalytic supports rather than others is responsible for different performances, in terms of both activity and selectivity. In this aim, if Ni is dispersed on Al_2O_3, especially in the low temperature range, dehydration reactions, followed by polymeric carbonate species formation, occurred [23]. On the contrary, by supporting Ni on rare earth oxides decreasing carbon formation rates were observed [24]. Ni/CeO_2 catalysts were shown to be very active towards ESR: nickel sites promote ethanol adsorption on the catalytic surface, while CeO_2 ensures water decomposition, allowing OH groups releasing, involved in CO_2 and H_2 formation. Moreover, high water-to-ethanol molar ratios avoid catalyst's deactivation due to the coke deposition on the catalytic surface, as only the production of filamentous carbon was favored [25]. Stoichiometric feeding conditions are also sufficient for obtaining relevant H_2 selectivity and a very low concentration of carbon monoxide [26]. The ESR promotion related to CeO_2 supports can be improved by adding proper dopants. In particular, for CeO_2-ZrO_2 based nickel catalysts, the effect of different metal loads was evaluated, showing a considerable amount of hydrogen also at low Ni percentages, probably due to the smaller particle metal size that promoted the metal-support interactions [27]. The combination of CeO_2 and ZrO_2 was also shown to promote ethanol reforming over Co based catalysts [28]. Moreover, investigations on Co/CeO_2 catalysts highlighted that the surface basification through calcium doping could be a possible route to increase the catalytic resistance to coke formation [29].

Catalytic activity of noble metals was also analyzed in depth [30-32]. Rhodium based catalysts were found to be very useful in reducing ethylene and acetaldehyde formation [33]. Moreover, by supporting Rh on ceria-zirconia based catalysts, the metal appeared to improve the CeO_2-ZrO_2 activity in oxidation reactions [34]. According to the literature, the promising performances of Pt based catalysts are related to their good thermal stability and high activity towards WGS reactions [35]. In the low temperature range (300-450°C), metal loading in the order of 1%wt was enough for limiting deactivation phenomena on CeO_2 supported catalysts. On the contrary, Pt/Al_2O_3 catalysts were much less selective towards WGS reaction, so resulting in lower H_2 and CO_2 production [36].

Although monometallic catalysts showed satisfactory performances for ethanol steam reforming, the development of bimetallic ones, which take advantage of the synergy between two metals, was the focus of many studies [37-40]. A strong influence of the preparation method on activity and selectivity of bimetallic PtCo or PtNi based catalysts supported on CeO_2 was observed. The impregnated samples showed higher performances with respect to the co-precipitated ones, ensuring a better agreement with thermodynamic equilibrium. Moreover, the impregnation order appeared crucial: the addition of the noble metal in the second impregnation step promoted ethanol adsorption and coke precursors hydrogenation [41].

Most of the works reported in literature deals with the use of powder catalysts for ethanol steam reforming. However, these catalytic systems may cause temperature and composition maldistributions and relevant pressure drop through the catalytic bed [42]. On the contrary, structured catalysts were shown to be very promising in order to overcome the serious powder's drawbacks. For example, the establishment of turbulent fluxes in the gaseous feedings, enhancing heat and mass transfer phenomena, was observed in the presence of high conductive catalytic foams[43, 44]. In particular, the comparison between the performances of foam and monolithic catalysts for methane auto-thermal reforming revealed that the former was able to flatten axial thermal profile ensuring higher catalytic activity, and reducing hot-spot phenomena [45].

Moreover, in the case of ESR, the catalytic system geometry, as well as the reactor configuration, plays a crucial role on the reformer performances, affecting the thermal management inside the reaction volume and, in turn, determining the temperature profile within catalytic bed [46].

In this work, catalytic performances of Pt-Ni/CeO_2 and Pt-Ni/CeO_2-ZrO_2 based catalysts for low-temperature steam reforming were investigated by studying both catalyst powders and catalytically coated SiC open-cell foams behaviour. Powder catalysts were tested in annular and tubular configuration, the latter employed also for structured samples; the results were compared with the aim of understanding potential ceramic foams property as catalyst carrier.

2. Experimental

2.1 Catalysts preparation and characterization

Nickel-Platinum based catalysts were prepared on CeO_2 and CeO_2-ZrO_2, both in powder and deposed on ceramic foams.

Powder catalysts were prepared by wet impregnation method [19]: platinum chloride (PtCl4) and nickel acetate ($C_4H_6O_4Ni*4H_2O$) (HPLC grade, supplied by Sigma-Aldrich) were selected as precursors of Pt and Ni respectively; CeO_2 (BET surface area 127 m^2/g) and CeO_2-ZrO_2 (BET surface area 64 m^2/g) were supplied by Rhodia. Nickel precursor salt was dissolved in bidistilled water and stirred at room temperature. Then the calcined support was added to the solution, and the impregnation was carried out on a stirring and heating plate up to the water vaporization. Then the catalyst was dried overnight (T = 120°C) and calcined in air at 600°C for 3 hours (heating rate 10°C/min). The following Platinum impregnation was performed by the same procedure. The catalyst preparation was setup to obtain 3%wt Pt /10%wt Ni on both the supports. Prepared samples were crushed and sieved in order to obtain a size distribution ranging between 180÷355 μm.

Structured catalysts were obtained by starting from silicon carbide foams (30 ppi, mean void fraction 85%), in a cylindrical shape sized D14.2 x 21.1 mm. SiC foams covered by ceria (203.5 g/l) or ceria-zirconia (170.9 g/l) washcoats. Foam preparation and coating were carried out at IKTS that developed a coating technology able to stabilize a homogeneous and thin washcoat layer on the ceramic foam without blocking the open-celled structure. The coating technology can be described as a combination of dip-coating and spin-coating. In the first step, the ceramic foam was dipped into the coating slurry, and then a vertical centrifuge was used to remove excessive slurry from the ceramic network. After drying and calcination steps, Ni and Pt deposition was realized in the ProCEED labs at University of Salerno. The washcoated foams were impregnated with an aqueous solution of the metal precursors (the same used for powders), at T= 60 °C for 1 hour; then the samples were dried at T= 120 °C for 2 hours and calcined for 1 hour at 400°C for Ni deposition and 550°C for Pt. The two different temperatures were selected on the basis of thermo-gravimetric analysis results (here not reported). The whole impregnation-drying-calcination procedure was repeated several times up to reach the desired amount of metal loading (3wt% for Pt and 10wt% for Ni). Total amounts of catalyst (washcoat + active species) deposed on the foam was 0.789 g for CeO_2 based sample and 0.548 g for CeO_2-ZrO_2 sample. As a final step, the sample was calcined in air at 600 °C for 3 hours, to stabilize it.

Specific area measurements were performed through N_2 adsorption at -196°C, carried out in a Sorptometer 1040 ‘‘Kelvin’’ from Costech Analytical Technologies. In order to release the eventual moisture from catalyst surface, before each analysis the samples were evacuated at 150°C for 1 hour in He flux.

Catalysts and supports diffraction patterns were produced by a D8 Brooker. The wavelength of the incident beam was 1.5406 Å and the incident angle ranged from 20 to 80 degree. Average crystallite sizes were determined by using Scherrer formula.

Raman analyses were performed through the Dispersive MicroRaman (Invia, Ranishaw) Spectroscope with a multilaser diode (514 nm) and a shift in frequency varying between 100 and 2000 cm^{-1}.

Temperature programmed reduction (TPR) measurements were carried out in the laboratory apparatus described in paragraph 2.2. The temperature was increased to 600°C with an heating rate of 20°C/min; a 5%H_2 in N_2 flow rate was used as reducing stream, ensuring a GHSV of 114350 h^{-1}.

2.2 Ethanol Steam Reforming tests

The laboratory plant, where catalytic tests were carried out, was previously described in details [19].

Powder and foam catalysts were tested in a tubular reactor (Figure 1); further tests on powder catalysts were performed in an annular reactor (Figure 2), in order to reduce heat transfer limitations and then thermal radial-gradient.

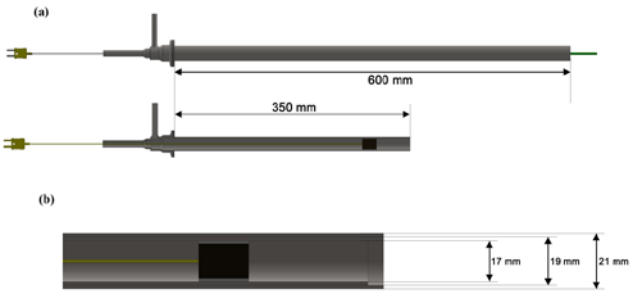

Figure 1: Hollow tubular reactor (a); details of catalytic section (b).

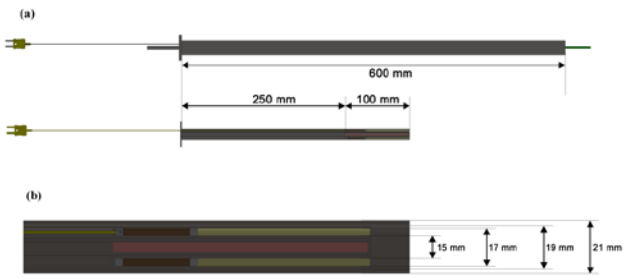

Figure 2: Annular tubular reactor (a); details of catalytic section (b).

Both the continuous fixed bed reactors (stainless steel, 19 mm i.d. and with a length 600 mm) were placed in a three zone electric oven. Thermic control in the different oven zones was realized through three temperature programmer-controller (TLK 43 by Tecnologic) connected to three "K type" thermocouples, detecting, respectively, inlet, middle and outlet oven sections, in order to assure a very flat thermal profile. Catalytic foams were held in place through a ceramic pad while catalytic powders were sandwiched between quartz flakes. System temperature was monitored in the catalytic volume by inserting a K-type thermocouple placed at the centre of the catalyst end section, while pressure was monitored in correspondence of the inlet section.

Reaction system was fed by ethanol and steam, moreover nitrogen was used as diluent. The H_2O/C_2H_5OH liquid mixture was delivered to the system through a Coriolis mass flow controller (Quantim, Brooks); the liquid stream was vaporized in a boiler before entering the reaction section. Nitrogen stream was delivered to the system by a mass-flow controller (5850 series, Brooks). The product composition was monitored by an on-line Nicolet Antaris IGS FT-IR multi-gas analyser, equipped with a heated gas cell, specifically designed with an optical path length of 12 cm, operating at temperature up to 185°C, and a MCT-A N_2 liquid-cooled detector. The FT-IR analyser allow monitoring the composition of CH_4, H_2O, CO, CO_2, C_2H_5OH (wet-base); the hydrogen and oxygen contents were determined by a thermoconductivity ABB-CALDOS 27 and a continuous paramagnetic analyser ABB-MAGNOS 206, respectively. In order to avoid any condensation between the reaction system and the FT-IR analyser, heating traces were used as connection; a cold trap placed between FT-IR and ABB analysers ensures gas drying, in order to save Magnos and Caldos detectors.

Catalytic tests were performed at atmospheric pressure in the temperature range 300÷600°C (from 600°C to 300°C @ 3°C/min), by feeding ethanol, steam and nitrogen ($C_2H_5OH:H_2O:N_2$ = 1:3:16, diluting ratio r.d. = 4 and feeding ratio r.a. = 3) with a GHSV of 114350 h^{-1}. For the powder samples tests, a mass of catalyst equal to the amount loaded on the respective foams was used (0.789 g for the CeO_2, 0.548 g for the CeO_2-ZrO_2), diluted with quartz (1:1 vol, 500÷710 μm) to reduce pressure drops.

3. Results and discussion

3.1 Catalysts characterization

BET analysis results carried out on fresh powder catalysts and bare supports and are listed in Table 1.

Table 1: Specific surface area (SSA) of supports and catalysts after calcination.

Sample	Support SSA [m^2/g]	Catalyst SSA [m^2/g]	SSA reduction [%]
Pt-Ni/CeO_2	127	72	43
Pt-Ni/CeO_2-ZrO_2	64	49	23

By comparing SSA of the two supports, it is possible to observe the higher ceria specific surface area with respect to ceria-zirconia. However, active species deposition causes a more evident SSA reduction in the case of Pt-Ni/CeO_2 (43% of reduction against 23% of bimetallic ceria-zirconia supported sample).

X-ray diffraction profiles of supports and catalysts are shown in Figure 3. All these patterns were compared with the database of the International Centre for Diffraction Data (ICDD). From XRD spectra of CeO_2 based samples, the typical peaks of ceria cubic fluorite structure are visible (at 2θ values of 28.542, 47.475 and 56.332°). Furthermore, the peaks related to NiO (ICDD file: 78-0643), identified at 37.265° and 43.298°, and 62.896°, can be detected in the profiles of both the catalysts. However, there are no PtO_x peaks, probably due to the high dispersion of noble metal and/or its low content.

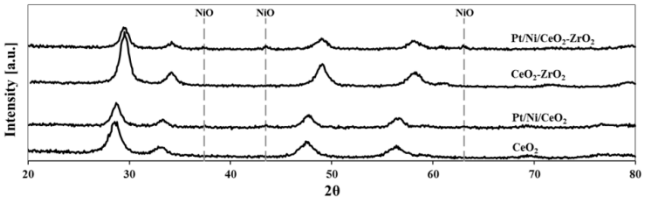

Figure 3: XRD spectra of supports and bimetallic catalysts after calcination.

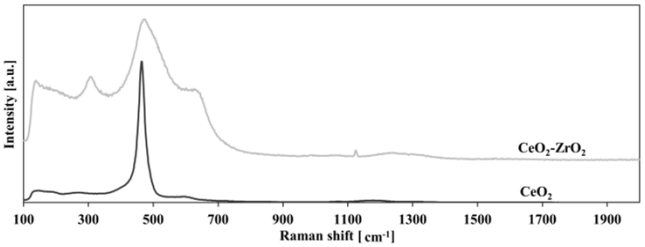

Figure 4: Raman spectra of ceria and ceria zirconia after calcination.

XRD patterns of ceria-zirconia based samples are very alike to the ceria ones. Nevertheless, a rightward peaks shift was observed. In order to perform deeper investigations on ceria-zirconia structure, the two supports were further characterized by Raman analysis.

In Figure 4, Raman spectra of CeO_2 and CeO_2-ZrO_2 were compared: the differences among the two lattices can be more easily highlighted. The introduction of Zr^{4+} ions in ceria crystalline structure induces a clear distortion of unit cell, due to the lower dimension of Zr^{4+} with respect to Ce^{4+} which is responsible for the formation of structural defects (like oxygen distortions) [47]. The oxygen relocation as a consequence of cell distortion makes tetragonal the ceria-zirconia crystalline structure.

The average crystallite dimensions of active species and support, calculated starting from XRD spectra by Scherrer formula, are reported in Table 2.

Table 2: Average sizes of the crystallites of the support and NiO.

Sample	<d> Support [Å]	<d> NiO [Å]
CeO_2	55	-
Pt-Ni/CeO_2	70	105
CeO_2-ZrO_2	69	-
Pt-Ni/CeO_2-ZrO_2	73	166

The deposition of active species increased support grains in both cases. Moreover, the higher dispersion of NiO on CeO_2 surface can be ascribed to the lower dimensions of support crystallites with respect to CeO_2-ZrO_2 ones.

Before ESR reaction, the bimetallic catalysts were activated in H_2 flux. The TPR profile of Pt-Ni/CeO_2 and Pt-Ni/CeO_2-ZrO_2 samples, deconvoluted after background subtraction by a least-squares fitting to Gaussian–Lorentzian functions using the software Microcal Origin, are presented, respectively, in Figure 5 and Figure 6.

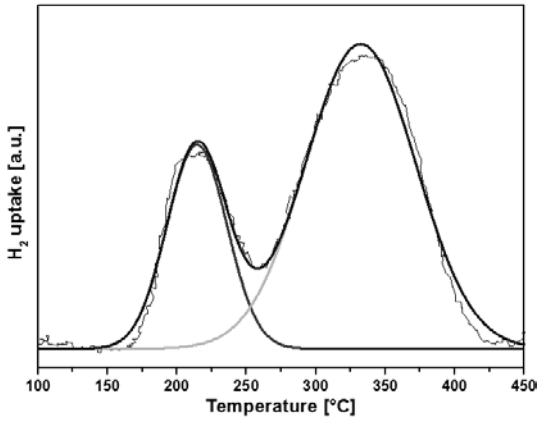

Figure 5: TPR profile of Pt-Ni/CeO_2

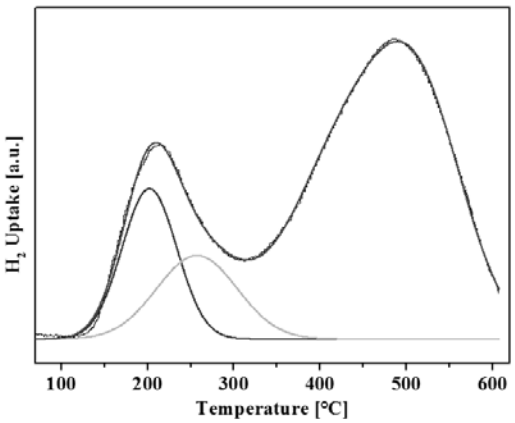

Figure 6: TPR profile of Pt-Ni/CeO_2-ZrO_2.

For the CeO_2 based sample, the lower peak temperature (T=214°C) can be related to PtO_2 species reduction, while the reduction peak of NiO was observed at 332°C. With respect to the literature predictions [48], the NiO peak was shifted at lower temperature, probably due to spillover phenomena, often observed in the presence of platinum [49, 50].

Lower reduction temperatures were observed for both PtO_2 and NiO (202 and 257°C, respectively) for the CeO_2-ZrO_2 supported catalyst. In fact, the ZrO_2incorporation in ceria lattice makes Ce^{4+} ions more active than the ceria alone toward redox reactions [51]. Moreover, spillover phenomena were shown to be more common in the case of ceria-zirconia [52].

Starting from the deconvoluted TPR profiles, the hydrogen uptake during the reduction was evaluated. The comparison between theoretical and experimental H_2 uptake is reported in Table 3.

The theoretical H_2 uptake due to the reduction of metal oxides was calculated according to the loading of active species.

Concerning ceria supported catalysts, Pt^{4+} reduction to Pt^0 involved the consumption of 624 $\mu molH_2/g_{cat}$, more than twice the theoretical one. This difference can be ascribed to the ability of Pt to promote hydrogen dissociation coupled with migration towards support surface and, as a result, its early reduction [53]. On the contrary, experimental and theoretical values were comparable for the NiO peak.

For ceria-zirconia samples, very different results were observed. In fact, the H_2 uptake related to PtO_2 reduction (2336 $\mu molH_2/g_{cat}$) was approximately one order of magnitude higher than the expected (308 $\mu molH_2/g_{cat}$).

Table 3: Quantitative analysis of H_2 uptake.

Sample	Species	T [°C]	Theoretical [μmol/g_{cat}]	Experimental [μmol/g_{cat}]
Pt-Ni/CeO_2	PtO_2	214	308	624
	NiO	332	1704	1710
Pt-Ni/CeO_2-ZrO_2	PtO_2	202	308	2336
	NiO	257	1704	1898

Also the consumption corresponding to $Ni^{2+} \rightarrow Ni^0$ reduction (1898 μmolH_2/g_{cat}) is slightly different from the theoretical uptake (1704 μmolH_2/g_{cat}). From these analysis, it is possible to state that the higher reducibility of ceria-zirconia support made H_2 spillover more evident with respect to ceria based samples. The enhanced spillover phenomena observed in the presence of both noble and non-noble metals, when dispersed on CeO_2-ZrO_2 supports, were in good agreement with results proposed in the literature [54].

3.2 Activity tests: effect of reactor configuration

Ceria supported samples were preliminarily tested at the operating conditions summarized in Table 4.

ESR reaction tests on powder sample were carried out in both annular and tubular configuration while the activated foam was tested in the tubular reactor.

Table 4: Operating conditions of activity tests.

r.a.	r.d	T [°C]	GHSV [h^{-1}]
3	4	300-600°C	114350

The three catalytic systems were compared in terms EtOH conversion (Figure 7) and H_2 yield (Figure 8) as a function of the mean gas temperature measured at the outlet of the catalytic bed.

By comparing powder catalyst tests, results confirmed the better performances of annular reactor, resulting in a higher ethanol conversion and an appreciable approach to thermodynamic equilibrium values, in terms of H_2 yield, in the whole temperature range. In fact, the annular configuration minimized temperature gradients in radial direction, ensuring an higher thermal control which is a critical issue for reforming reactions [46]. As a consequence, higher heat flux was assured between energy source (e.g. the oven) and reaction volume, resulting in improved reaction rates. On the contrary, lower heat fluxes and more difficult thermal control are typical of tubular reformers [55]. The worst performances recorded in the tubular reactor may be exactly linked to the non-uniform thermal distribution, resulting in a very low heat transfer from external heat source to catalytic bed. As a consequence, H_2 yields lower than 50% even at 600°C and incomplete ethanol conversion in the entire temperature range were recorded.

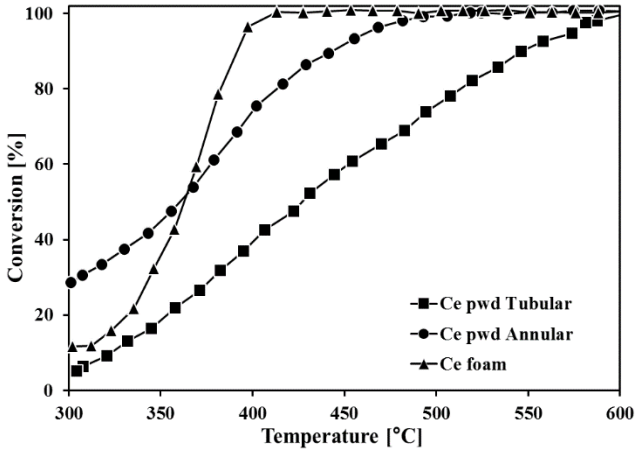

Figure 7: Ethanol conversions (*X*) for CeO_2 based catalysts as a function of temperature; total flow rate = 835 Ncm^3/min, GHSV = 114350 h^{-1}.

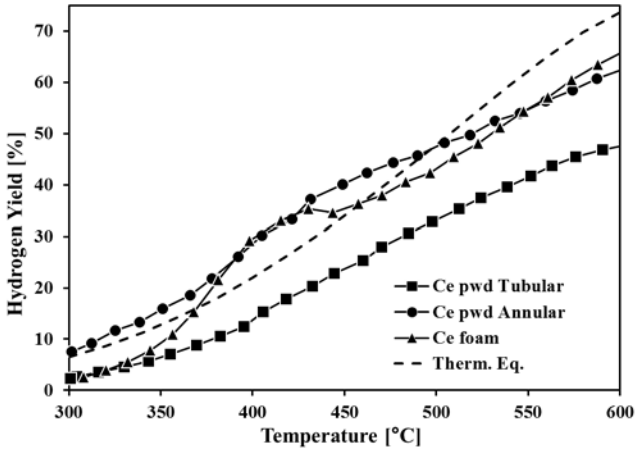

Figure 8: Hydrogen yields (*Y*) for CeO_2 based catalysts as a function of temperature; total flow rate = 835 Ncm^3/min, GHSV = 114350 h^{-1}.

Foam catalyst tested in tubular reactor showed very interesting results, as at T>500°C foam tubular and powder annular profiles were overlapping (Figure 7). Furthermore, foams reached the highest EtOH conversion at temperature above 360°C (total ethanol conversion above 400°C), moreover H_2 yields were comparable with what observed in the annular configuration. The optimal thermal conductivity of silicon carbide, in fact, decreased the typical heat transfer limitation of the tubular reactor, assuring a more uniform radial temperature [56]. In addition, the foams geometry was able to impose a chaotic flux to reactant mixture, enhancing heat and mass transfer rates [57, 58].

Taking into account the unsatisfactory results observed for powders in the tubular reactor configuration, further investigations were focused on powder samples tested in the only annular reactor, and foams tested in the tubular reactor.

3.3 *Activity tests: effect of catalytic support*

The influence of catalytic supports (ceria and ceria-zirconia) on ESR activity was also studied and results obtained in terms of ethanol conversion and hydrogen yield are reported in Figure 9 and Figure 10 respectively. The operating conditions were the same reported in Section 3.2.

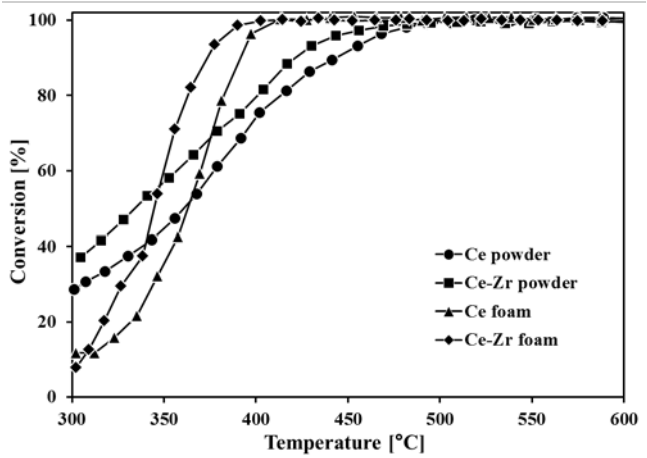

Figure 9: Ethanol conversion for CeO_2 and CeO_2-ZrO_2 based catalysts as a function of temperature; GHSV=114350 h^{-1}.

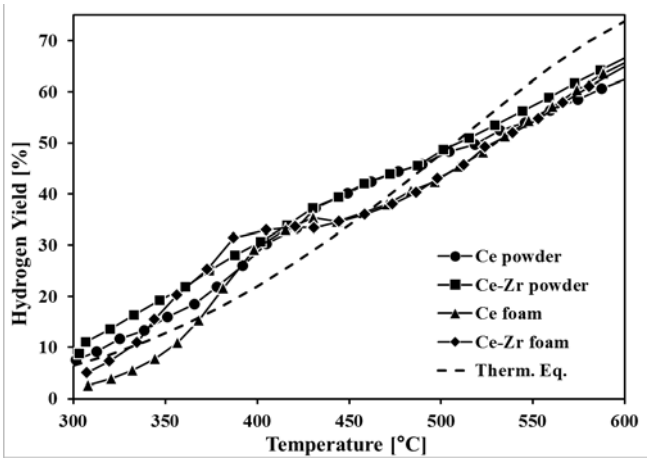

Figure 10: Hydrogen yield (*Y*) for CeO_2 and CeO_2-ZrO_2 based catalysts as a function of temperature; GHSV=114350 h^{-1}.

At $T > 500$°C, total ethanol conversions were recorded for all the tested samples. Reducing temperature, lower conversions were reached in the presence of powder catalysts while foams samples were shown to be more active for *T* ranging from 500 and 350°C. Only in a very small range (300-350°C) powders tested in the annular reactor ensured better performances than foams.

By comparing CeO_2 and CeO_2-ZrO_2 based catalysts in terms of activity, it is possible to observe the more interesting results reachable in the latter case, for both powders and foams samples. The worst performances recorded for CeO_2 based samples may be ascribed to a catalyst deactivation during the activity screening. In fact, ceria-zirconia solid solutions, when optimized, as in the present study, in terms of Ce/Zr molar ratios (close to 1) [59], are characterized by oxygen storage and release properties higher than ceria alone, thus enhancing coke gasification reactions and limiting deactivation in a wider temperature range (Figure 9).

The performances of foam catalysts, in terms of H_2 yields, were very similar at $T > 420$°C (Figure 10). However, at lower temperatures, H_2 production is higher in the presence of ceria-zirconia. In this case, in fact, WGS reaction was enhanced, due to the better oxygen storage capacity. The very pronounced H_2 yield hump, recorded over both the foam catalysts between 350 and 450°C, can be ascribed to the higher activity of these samples towards CH_4 steam reforming. Also for powder catalysts very similar H_2 yields values were recorded, especially in the middle temperature range (*T* ranging from 400 and 500°C). The better results recorded at $T < 500$°C over Pt-Ni/CeO_2-ZrO_2 powder highlighted the ability of the support in promoting ethanol reforming reaction.

The very promising activity of ceria-zirconia based catalysts to produce H_2 via ethanol steam reforming was in well agreement with recent literary studies [28, 60].

3.4 *Activity tests: effect of space velocity*

The effect of space velocity on activity of bimetallic catalysts was investigated varying GHSV (100000÷400000 h^{-1}) and analysing ethanol conversion and hydrogen yield at two different temperatures, 450 and 500°C.

The results, reported in terms of ethanol conversion, are shown in Figure 11 and Figure 12.

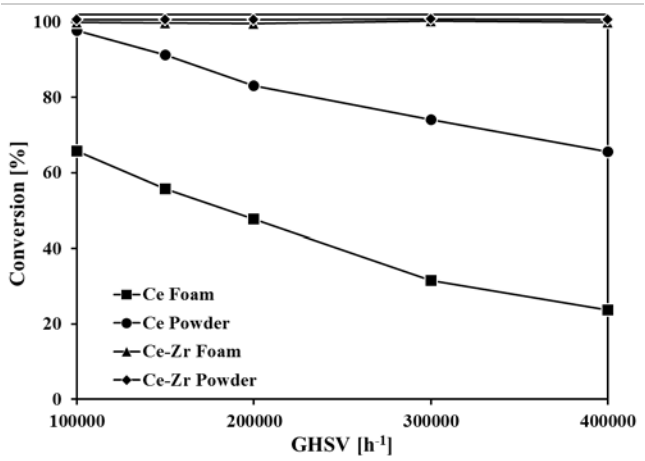

Figure 11: Ethanol conversion as a function of GHSV at 450°C.

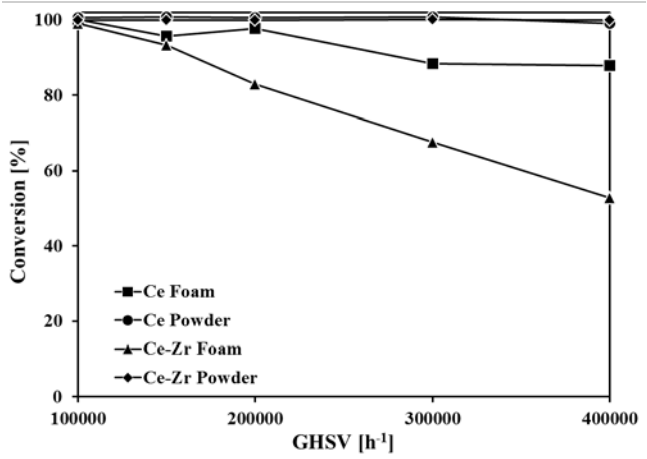

Figure 12: Ethanol conversion as a function of GHSV at 500°C

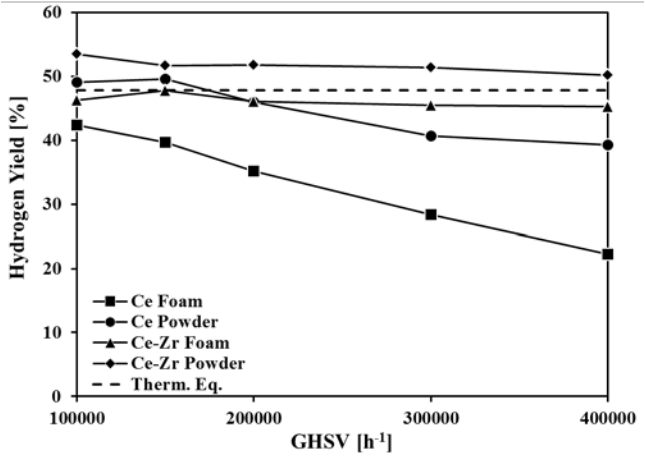

Figure 14: Hydrogen yield as a function of GHSV at 500°C.

Both powder and foam Pt-Ni/CeO_2-ZrO_2 catalysts reached total ethanol conversions, and these values were affected by neither space velocity increase nor temperature decrease. On the contrary, less interesting results were recorded over ceria based catalysts, whose conversion decreased with an increase in space velocity. For powder sample, C_2H_5OH conversion varied from 100% to 88% at 500°C (Figure 11) while at lower temperature a more evident reduction was observed (65% at 400000 h^{-1}). Pt-Ni/CeO_2 foam showed the worse performances, appearing heavily influenced by contact time decrease: the very promising catalyst performances observed at 100000 h^{-1} and 500°C, collapsed for the lowest contact time tests. Lowering T, the influence of deactivation phenomena became higher and only 24% of conversion was reached at 400000 h^{-1} (Figure 12).

The comparison between experimental and equilibrium (dotted line) H_2 yields is presented in Figure 13 and Figure 14.

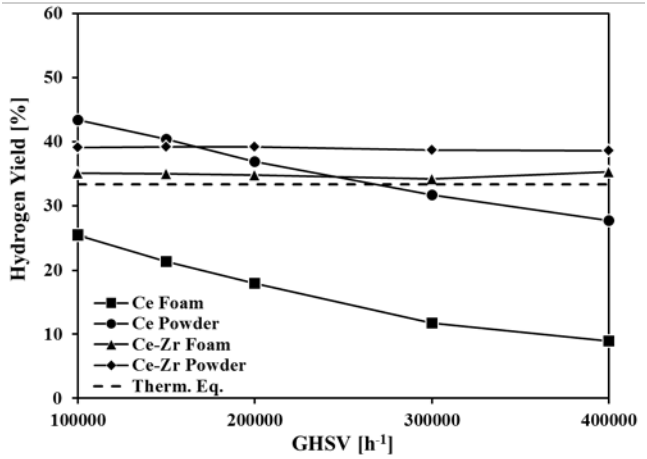

Figure 13: Hydrogen yield as a function of GHSV at 450°C.

Ceria-zirconia based catalysts, at both the investigated temperatures, showed, when space velocity was increased, very little changes in H_2 yields. At 500°C, H_2 yields recorded over activated ceria-zirconia foams exceeded the equilibrium value (48%) in the whole investigated GHSV range, while powders reached H_2 yields lower than thermodynamic ones at a space velocity higher than 150000 h^{-1}. When activity tests were performed at 450°C, the catalysts supported over ceria-zirconia ensured H_2 production rates superior than 34% (equilibrium value) at every investigated contact time. This is probably related to the lower temperature and the very high space velocities employed, at which catalysts were less active towards methanation reaction. Pt-Ni/CeO_2 powders performances were interesting for relatively low space velocity values, independently from reaction temperature, while for ceria foams very low H_2 production rates were observed in the entire space velocity investigated range. The H_2 yields reduction, observed for all the samples when T moved from 500 to 450°C, can be attributed to the decreased steam reforming activity, due in turn to the endothermic reaction.

3.5 Stability tests

Pt-Ni/CeO_2-ZrO_2 samples, which showed the better results in terms of both ethanol conversion and hydrogen yield, were also employed for stability tests, carried out at 100000 h^{-1} and 450°C. The latter stressful temperature was selected to eventually accelerate deactivation times.

Times on stream tests (TOS) results, showed in terms of volumetric products distribution versus time, are reported in Figure 15 and Figure 16. These profiles were compared with equilibrium concentrations.

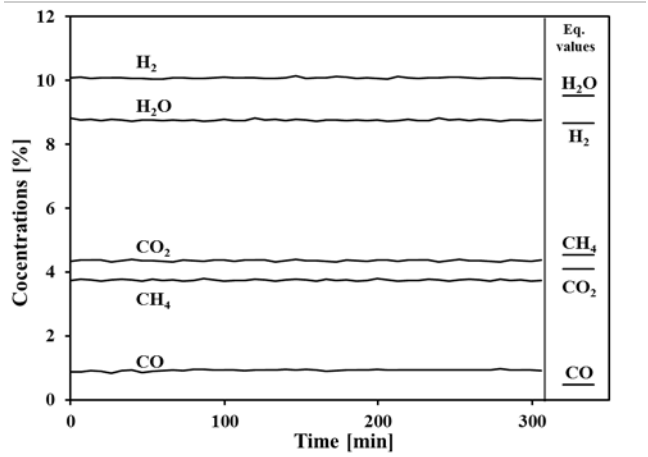

Figure 15: TOS test over Pt-Ni/CeO_2-ZrO_2 powder; GHSV=100000 h^{-1} and T=450°C

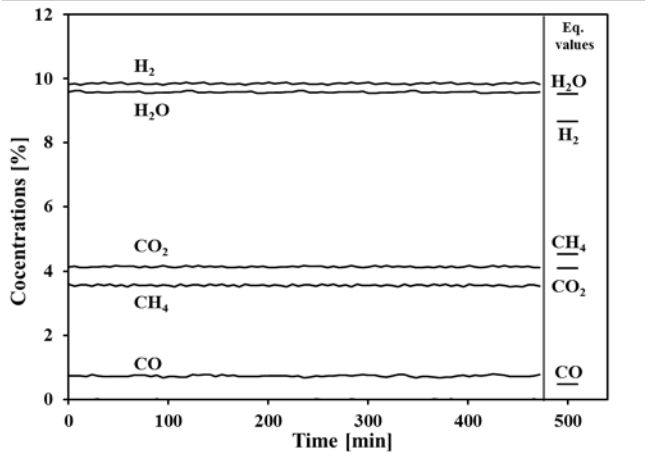

Figure 16: TOS test over Pt-Ni/CeO_2-ZrO_2 foam; GHSV=100000 h^{-1} and T=450°C

Both the samples appeared very stable and no apparent deactivation phenomena were evident since the product distribution was not affected during the time on stream (TOS).

From volumetric products distribution, powder catalyst appeared more active towards steam reforming reactions, ensuring CO_2 and H_2O concentrations respectively higher and lower than equilibrium ones. As CO levels recorded in reforming mixture were slightly lower when durability test was performed over catalytic foams, water gas shift reaction was probably more favoured over the structured sample.

3.6 Reactor configuration and heat transfer

The results presented so far provided an interesting overview of the heat transfer open-cell ceramic foams properties, able to ensure a more uniform radial profile in the tubular configuration, thus achieving performances comparable with the ones observed in the case of powders tested in the annular reactor.

In order to evaluate the heat transfer rate from the heating medium (the furnace) and the reaction volume occurring with the two CeO_2-ZrO_2 catalytic systems (annular-powder, tubular-foam), the oven set-point temperature was recorded for the 450°C tests. The difference between set-point (T_s) and catalysts (T_b) temperatures results proportional to thermal transport resistance. The investigation was carried out by increasing GHSV from 100000 to 400000 h^{-1}.

In Table 5 the set point temperatures fixed during stability tests, performed over ceria-zirconia based samples at T=450°C and at different contact times, were reported.

When catalytic foams were employed, a sensible reduction of the difference between T_s and T_b (almost 30%) was observed, showing the better thermal management of structured catalysts. Moreover, T_s was less affected by flow rates variation with respect to the powder.

From these analysis, is possible to demonstrate the very impressive thermal properties of SiC open cells ceramic foams [61, 62], able to reach a more stable thermic profile inside the catalytic bed, thus minimizing thermal transfer resistance. Moreover, economic impact of process can be in turn reduced, due to the lower temperature required for the heating medium.

Table 5: T_s values at different space velocities for Pt-Ni/CeO_2-ZrO_2 catalysts; T=450°C.

Sample	GHSV [h^{-1}]	T_s [°C]
Powder	100000	479
	200000	480
	300000	481
	400000	482
Foam	100000	471
	200000	471
	300000	472
	400000	472

4. Conclusions

Preliminary studies on structured bimetallic catalysts based on Pt-Ni/CeO_2 and Pt-Ni/CeO_2-ZrO_2, employed for low temperature ESR, were reported. Results confirmed the interesting behaviour of the catalytic formulations, since very appreciable ethanol conversions and hydrogen yields were observed despite the contact time applied was quite low. The promising performances observed in highly severe operating conditions (T < 500°C; GHSV > 100000 h^{-1}) suggest good resistance of catalytic formulations to deactivation phenomena. In particular, the role of the support was highlighted, underlining that the catalyst reducibility, promoted by catalytic substrate, improves the reforming reactions rate. Tests carried out on different reactor geometry evidenced the role of temperature management in the catalytic volume on the system performances. The high GHSV values resulted in a heat transfer limited process, since the powder catalyst showed good performances only in an optimized annular reactor able to lower radial thermal gradient. On the other hand, structured catalyst

prepared on open-cells SiC foams exploits SiC foam heat transfer properties, showing high performances (in term of both ethanol conversion and hydrogen yield) in a very easy tubular reactor geometry. The comparison of bimetallic ceria supported catalysts with ceria-zirconia ones displayed the more promising results of the latter catalytic formulation, mainly due to its enhanced oxygen storage and release properties.

Further investigations will be focused on coke formation tendency and long term stability (time on stream of more than one hundred hours) of catalytic foams.

References

[1] Haryanto A, Fernando S, Murali N, Adhikari S. Current status of hydrogen production techniques by steam reforming of ethanol: a review. Energy & Fuels. 2005;19:2098-106.

[2] Venkata Mohan S, Vijaya Bhaskar Y, Murali Krishna P, Chandrasekhara Rao N, Lalit Babu V, Sarma PN. Biohydrogen production from chemical wastewater as substrate by selectively enriched anaerobic mixed consortia: Influence of fermentation pH and substrate composition. International Journal of Hydrogen Energy. 2007;32:2286-95.

[3] Kırtay E. Recent advances in production of hydrogen from biomass. Energy Conversion and Management. 2011;52:1778-89.

[4] Llorca J, de la Piscina PRr, Dalmon J-A, Sales J, Homs Ns. CO-free hydrogen from steam-reforming of bioethanol over ZnO-supported cobalt catalysts: Effect of the metallic precursor. Applied Catalysis B: Environmental. 2003;43:355-69.

[5] Aupretre F, Descorme C, Duprez D, Casanave D, Uzio D. Ethanol steam reforming over MgxNi1−xAl2O3 spinel oxide-supported Rh catalysts. Journal of Catalysis. 2005;233:464-77.

[6] Lima da Silva A, Malfatti CdF, Müller IL. Thermodynamic analysis of ethanol steam reforming using Gibbs energy minimization method: A detailed study of the conditions of carbon deposition. International Journal of Hydrogen Energy. 2009;34:4321-30.

[7] Fierro V, Akdim O, Provendier H, Mirodatos C. Ethanol oxidative steam reforming over Ni-based catalysts. Journal of Power Sources. 2005;145:659-66.

[8] Benito M, Sanz JL, Isabel R, Padilla R, Arjona R, Daza L. Bio-ethanol steam reforming: Insights on the mechanism for hydrogen production. Journal of Power Sources. 2005;151:11-7.

[9] Wang W, Wang Y. Thermodynamic analysis of hydrogen production via partial oxidation of ethanol. International Journal of Hydrogen Energy. 2008;33:5035-44.

[10] Ioannides T. Thermodynamic analysis of ethanol processors for fuel cell applications. Journal of Power Sources. 2001;92:17-25.

[11] Vaidya PD, Rodrigues AE. Insight into steam reforming of ethanol to produce hydrogen for fuel cells. Chemical Engineering Journal. 2006;117:39-49.

[12] Mas V, Kipreos R, Amadeo N, Laborde M. Thermodynamic analysis of ethanol/water system with the stoichiometric method. International Journal of Hydrogen Energy. 2006;31:21-8.

[13] Fatsikostas AN, Kondarides DI, Verykios XE. Steam reforming of biomass-derived ethanol for the production of hydrogen for fuel cell applications. Chemical Communications. 2001:851-2.

[14] Akande AJ, Idem RO, Dalai AK. Synthesis, characterization and performance evaluation of Ni/Al2O3 catalysts for reforming of crude ethanol for hydrogen production. Applied Catalysis A: General. 2005;287:159-75.

[15] Llorca J, Homs Ns, Sales J, de la Piscina PRr. Efficient Production of Hydrogen over Supported Cobalt Catalysts from Ethanol Steam Reforming. Journal of Catalysis. 2002;209:306-17.

[16] Batista MS, Santos RKS, Assaf EM, Assaf JM, Ticianelli EA. High efficiency steam reforming of ethanol by cobalt-based catalysts. Journal of Power Sources. 2004;134:27-32.

[17] Breen JP, Burch R, Coleman HM. Metal-catalysed steam reforming of ethanol in the production of hydrogen for fuel cell applications. Applied Catalysis B: Environmental. 2002;39:65-74.

[18] Mattos LV, Noronha FB. Hydrogen production for fuel cell applications by ethanol partial oxidation on Pt/CeO2 catalysts: the effect of the reaction conditions and reaction mechanism. Journal of Catalysis. 2005;233:453-63.

[19] Palma V, Castaldo F, Ciambelli P, Iaquaniello G. Hydrogen production through catalytic low-temperature bio-ethanol steam reforming. Clean Techn Environ Policy. 2012;14:973-87.

[20] Kazama A, Sekine Y, Oyama K, Matsukata M, Kikuchi E. Promoting effect of small amount of Fe addition onto Co catalyst supported on α-Al2O3 for steam reforming of ethanol. Applied Catalysis A: General. 2010;383:96-101.

[21] Muroyama H, Nakase R, Matsui T, Eguchi K. Ethanol steam reforming over Ni-based spinel oxide. International Journal of Hydrogen Energy. 2010;35:1575-81.

[22] Hyman MP, Vohs JM. Reaction of ethanol on oxidized and metallic cobalt surfaces. Surface Science. 2011;605:383-9.

[23] Fatsikostas AN, Verykios XE. Reaction network of steam reforming of ethanol over Ni-based catalysts. Journal of Catalysis. 2004;225:439-52.

[24] Wang L, Li D, Koike M, Watanabe H, Xu Y, Nakagawa Y, et al. Catalytic performance and characterization of Ni–Co catalysts for the steam reforming of biomass tar to synthesis gas. Fuel. 2013;112:654-61.

[25] Xu W, Liu Z, Johnston-Peck AC, Senanayake SD, Zhou G, Stacchiola D, et al. Steam Reforming of Ethanol on Ni/CeO2: Reaction Pathway and Interaction between Ni and the CeO2 Support. ACS Catalysis. 2013;3:975-84.

[26] Fajardo H, Probst LD, Carreño NV, Garcia IS, Valentini A. Hydrogen Production from Ethanol Steam Reforming Over Ni/CeO2 Nanocomposite Catalysts. Catal Lett. 2007;119:228-36.

[27] Ebiad MA, Abd El-Hafiz DR, Elsalamony RA, Mohamed LS. Ni supported high surface area CeO2-ZrO2 catalysts for hydrogen production from ethanol steam reforming. RSC Advances. 2012;2:8145-56.

[28] Lin SY, Kim D, Ha S. Hydrogen Production from Ethanol Steam Reforming Over Supported Cobalt Catalysts. Catal Lett. 2008;122:295-301.

[29] Pang X, Chen Y, Dai R, Cui P. Co/CeO2 Catalysts Prepared Using Citric Acid Complexing for Ethanol Steam Reforming. Chinese Journal of Catalysis. 2012;33:281-9.

[30] Erdőhelyi A, Raskó J, Kecskés T, Tóth M, Dömök M, Baán K. Hydrogen formation in ethanol reforming on supported noble metal catalysts. Catalysis Today. 2006;116:367-76.

[31] Wanat EC, Venkataraman K, Schmidt LD. Steam reforming and water–gas shift of ethanol on Rh and Rh–Ce catalysts in a catalytic wall reactor. Applied Catalysis A: General. 2004;276:155-62.

[32] Cai W, Wang F, van Veen A, Descorme C, Schuurman Y, Shen W, et al. Hydrogen production from ethanol steam reforming in a micro-channel reactor. International Journal of Hydrogen Energy. 2010;35:1152-9.

[33] Freni S. Rh based catalysts for indirect internal reforming ethanol applications in molten carbonate fuel cells. Journal of Power Sources. 2001;94:14-9.

[34] Roh H-S, Wang Y, King D, Platon A, Chin Y-H. Low Temperature and H2 Selective Catalysts for Ethanol Steam Reforming. Catal Lett. 2006;108:15-9.

[35] Navarro RM, Álvarez-Galván MC, Sánchez-Sánchez MC, Rosa F, Fierro JLG. Production of hydrogen by oxidative reforming of ethanol over Pt catalysts supported on Al2O3 modified with Ce and La. Applied Catalysis B: Environmental. 2005;55:229-41.

[36] Ciambelli P, Palma V, Ruggiero A. Low temperature catalytic steam reforming of ethanol. 1. The effect of the support on the activity and stability of Pt catalysts. Applied Catalysis B: Environmental. 2010;96:18-27.

[37] Araque M, Vargas JC, Zimmermann Y, Roger A-C. Study of a CeZrCoRh mixed oxide for hydrogen production by ethanol steam reforming. International Journal of Hydrogen Energy. 2011;36:1491-502.

[38] Barroso MN, Gomez MF, Arrúa LA, Abello MC. CoZnAl catalysts for ethanol steam reforming reaction. Chemical Engineering Journal. 2010;158:225-32.

[39] Romero A, Jobbágy M, Laborde M, Baronetti G, Amadeo N. Ni(II)–Mg(II)–Al(III) catalysts for hydrogen production from ethanol steam reforming: Influence of the activation treatments. Catalysis Today. 2010;149:407-12.

[40] Sau GS, Bianco F, Lanchi M, Liberatore R, Mazzocchia CV, Spadoni A, et al. Cu–Zn–Al based catalysts for low temperature bioethanol steam reforming by solar energy. International Journal of Hydrogen Energy. 2010;35:7280-7.

[41] Palma V, Castaldo F, Ciambelli P, Iaquaniello G, Capitani G. On the activity of bimetallic catalysts for ethanol steam reforming. International Journal of Hydrogen Energy. 2013;38:6633-45.

[42] Cybulski A, Moulijn JA. Structured Catalysts and Reactors. Boca Raton, FL: CRC Press; 2005.

[43] Twigg MV, Richardson JT. Theory and Applications of Ceramic Foam Catalysts. Chemical Engineering Research and Design. 2002;80:183-9.

[44] Peng Y, Richardson JT. Properties of ceramic foam catalyst supports: one-dimensional and two-dimensional heat transfer correlations. Applied Catalysis A: General. 2004;266:235-44.

[45] Palma V, Ricca A, Ciambelli P. Fuel cell feed system based on H2 production by a compact multi-fuel catalytic ATR reactor. International Journal of Hydrogen Energy. 2013;38:406-16.

[46] Torres JA, Montané D. Model for Steam Reforming of Ethanol Using a Catalytic Wall Reactor COMSOL Conference. Hannover2008.

[47] Petkovich ND, Rudisill SG, Venstrom LJ, Boman DB, Davidson JH, Stein A. Control of Heterogeneity in Nanostructured Ce1−xZrxO2 Binary Oxides for Enhanced Thermal Stability and Water Splitting Activity. The Journal of Physical Chemistry C. 2011;115:21022-33.

[48] Woo Ryu J, Moon DJ, Lee SD, Lee B, G. , Hong S, I. . Catalytic properties of Pt-Ni/CeO_2 catalyst for WGS reaction. Theories and Application of Chemical Engineering. 2004;10:1024-7.

[49] Panagiotopoulou P, Papavasiliou J, Avgouropoulos G, Ioannides T, Kondarides DI. Water–gas shift activity of doped Pt/CeO2 catalysts. Chemical Engineering Journal. 2007;134:16-22.

[50] Lueking AD, Yang RT. Hydrogen spillover to enhance hydrogen storage—study of the effect of carbon physicochemical properties. Applied Catalysis A: General. 2004;265:259-68.

[51] Saidina Amin NA, Chong CM. SCR of NO with C3H6 in the presence of excess O2 over Cu/Ag/CeO2-ZrO2 catalyst. Chemical Engineering Journal. 2005;113:13-25.

[52] Takeguchi T, Furukawa S-n, Inoue M. Hydrogen Spillover from NiO to the Large Surface Area CeO2–ZrO2 Solid Solutions and Activity of the NiO/CeO2–ZrO2 Catalysts for Partial Oxidation of Methane. Journal of Catalysis. 2001;202:14-24.

[53] Laguna OH, Centeno MA, Romero-Sarria F, Odriozola JA. Oxidation of CO over gold supported on Zn-modified ceria catalysts. Catalysis Today. 2011;172:118-23.

[54] Norman A, Perrichon V, Bensaddik A, Lemaux S, Bitter H, Koningsberger D. Study of the Reducibility of Pt or Pd on Ceria–Zirconia Catalysts by XANES Measured at the Ce LIII Edge and Magnetic Susceptibility Measurements. Topics in Catalysis. 2001;16-17:363-8.

[55] Marigliano G, Barbieri G, Drioli E. Effect of energy transport on a palladium-based membrane reactor for methane steam reforming process. Catalysis Today. 2001;67:85-99.

[56] Palma V, Ricca A, Ciambelli P. Monolith and foam catalysts performances in ATR of liquid and gaseous fuels. Chemical Engineering Journal. 2012;207–208:577-86.

[57] Lacroix M, Nguyen P, Schweich D, Pham Huu C, Savin-Poncet S, Edouard D. Pressure drop measurements and modeling on SiC foams. Chemical Engineering Science. 2007;62:3259-67.

[58] Maestri M, Beretta A, Groppi G, Tronconi E, Forzatti P. Comparison among structured and packed-bed reactors for the catalytic partial oxidation of CH4 at short contact times. Catalysis Today. 2005;105:709-17.

[59] Aneggi E, Boaro M, Leitenburg Cd, Dolcetti G, Trovarelli A. Insights into the redox properties of ceria-based oxides and their implications in catalysis. Journal of Alloys and Compounds. 2006;408–412:1096-102.

[60] Biswas P, Kunzru D. Steam reforming of ethanol for production of hydrogen over Ni/CeO–ZrO catalyst: Effect of support and metal loading. International Journal of Hydrogen Energy. 2007;32:969-80.

[61] Twigg MV, Richardson JT. Fundamentals and Applications of Structured Ceramic Foam Catalysts. Industrial & Engineering Chemistry Research. 2007;46:4166-77.

[62] Coquard R, Loretz M, Baillis D. Conductive Heat Transfer in Metallic/Ceramic Open-Cell Foams. Advanced Engineering Materials. 2008;10:323-37.